LEGIBILITY NOTICE

A major purpose of the Technical Information Center is to provide the broadest dissemination possible of information contained in DOE's Research and Development Reports to business, industry, the academic community, and federal, state and local governments.

Although a small portion of this report is not reproducible, it is being made available to expedite the availability of information on the research discussed herein.

1

TITLE: STRAIN HARDENING AT LARGE STRAINS

AUTHOR(S): Anthony D. Rollett, MST-6
U. Fred Kocks, CMS
J. David Embury, McMaster univ.
Michael G. Stout, MST-5
Roger D. Doherty, Drexel Univ.

DISCLAIMER

Los Alamos
Los Alamos National Laboratory
Los Alamos, New Mexico 87545

STRAIN HARDENING AT LARGE STRAINS

A. D. Rollett, U. F. Kocks, J. D. Embury[†], M. G. Stout and R. D. Doherty[*]

Los Alamos National Laboratory, New Mexico 87545, USA

[†]McMaster University, Hamilton, Ontario, Canada

[*]Drexel University, Philadelphia, Pennsylvania, USA

ABSTRACT

The strain hardening properties of various f.c.c. metals have been investigated at large strains by means of torsion tests of short thin-walled cylinders. The results show that Stage IV occurs in all cases provided that a low enough test temperature is used; it is a nearly constant hardening rate of 2.10^{-4} G in terms of resolved flow stress. Stage IV strain hardening has been modeled by considering the effects of accumulation of dislocation debris, such as dipoles and loops, on the "saturation" stress. The "saturation" stress that can be obtained by extrapolation of Stage III is now a limiting flow stress that slowly increases with the accumulation of debris. The model reproduces the sharp transition from Stage III to Stage IV that occurs experimentally at low temperatures and, for a reasonable choice of parameters, the rate of hardening in Stage IV.

KEYWORDS

Strain Hardening; Stage IV; f.c.c. metals; work hardening; two-phase; single phase; hardening; torsion; temperature; strain rate.

INTRODUCTION

An investigation was made of the strain hardening properties of f.c.c. metals at large strains. This region of the stress-strain curve is commonly known as Stage IV after the classification introduced by Diehl (1956). The experimental characteristic of this stage in single phase materials is that of a linear stress-strain curve that follows the usual parabolic low-strain behavior. The classic observation was that of Langford and Cohen (1969) for wire-drawn iron but a better approach is that of the torsion test as shown by Kovacs and Feltham (1963) for silver. For two-phase materials the hardening rate appears to increase during Stage IV instead of remaining constant, as shown schematically in Fig. 1. Experimental data for over-aged Al-4Cu and the wire-drawing data of Bevk (1983), Fig. 2., support this view. Single-phase materials behave differently; Stage IV occurs in all f.c.c. metals, provided that a low enough test temperature is used, and the hardening rate is essentially constant in Stage IV, Fig. 3. Previous reviews by Gil-Sevillano et al. (1981) and by Hecker and Stout (1982) focussed on such features of large-strain deformation as the development of strong crystallographic textures and macroscopic heterogeneities in plastic flow. These appear to be adjuncts of large-strain plasticity but not the cause of sustained hardening, Rollett et al. (1988). This paper describes experimental data for single phase alloys together with models for single- and two-phase materials.

Traditional torsion tests used solid bars which lead to problems of interpretation because of the non-uniform strain inherent in the specimen design. The experiments described here

used the Lindholm (1980) specimen, which is a short thin-walled tube that permits the assumption of uniform strain and stress over the gauge section. The specimen is also stable to large strains because of the constraint of the relatively massive grip ends.
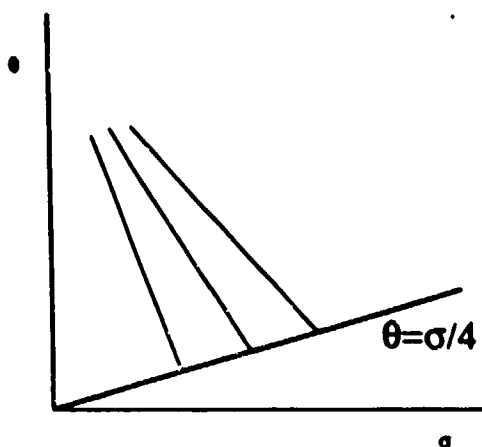

Fig. 1. Diagram of hardening rate versus stress for two-phase alloys, showing rising hardening rate in Stage IV.
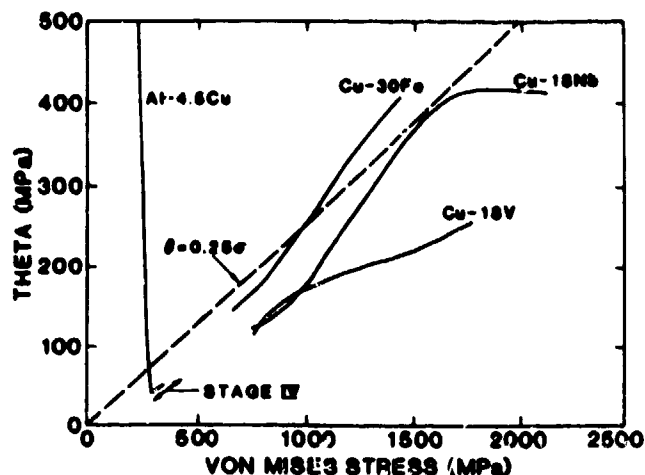

Fig. 2. Hardening rate versus stress for an over-aged Al-4w/o Cu and various Cu alloys, Bevk (1983).

Comparing the results for aluminum, copper and silver, Fig. 4, shows that Stage IV occurs at approximately the same rate for a wide range of stacking fault energy (SFE) to modulus (G) ratios. The plot was produced by taking the slope of the stress-strain curve and dividing by the appropriate Taylor factor (1.55 for torsion, Rollett, 1987) and shear modulus. This puts the data in terms of slip on a single slip plane and brings different materials onto approximately the same scale.
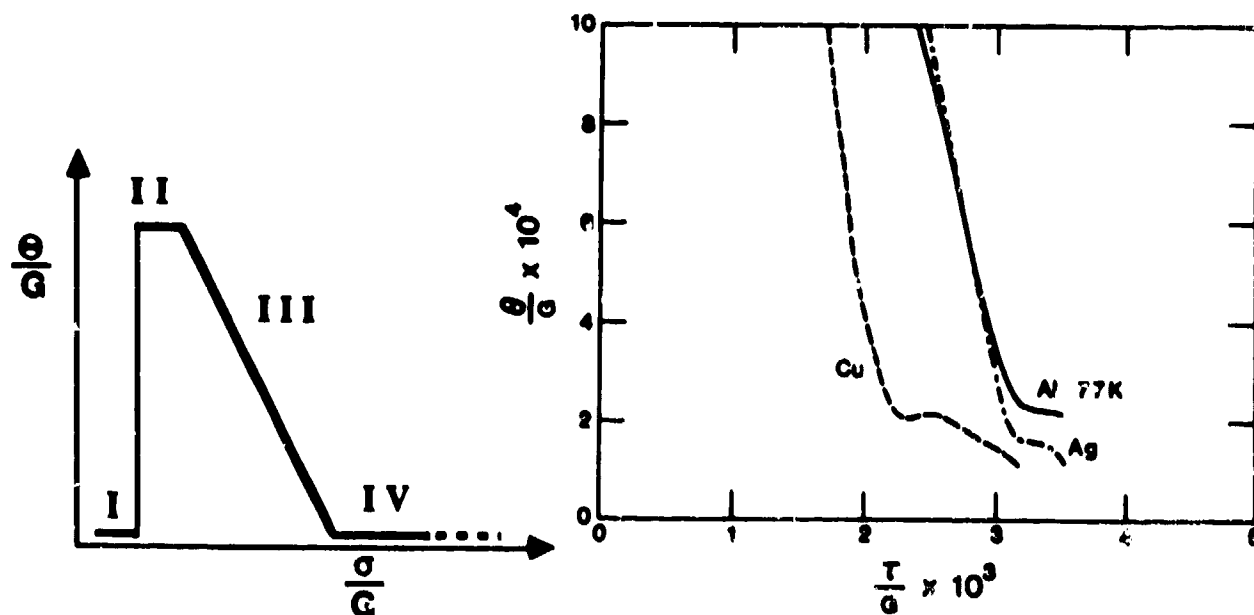

Fig. 3. Diagram of hardening rate versus stress for single-phase alloys, showing low and constant hardening rate in Stage IV.
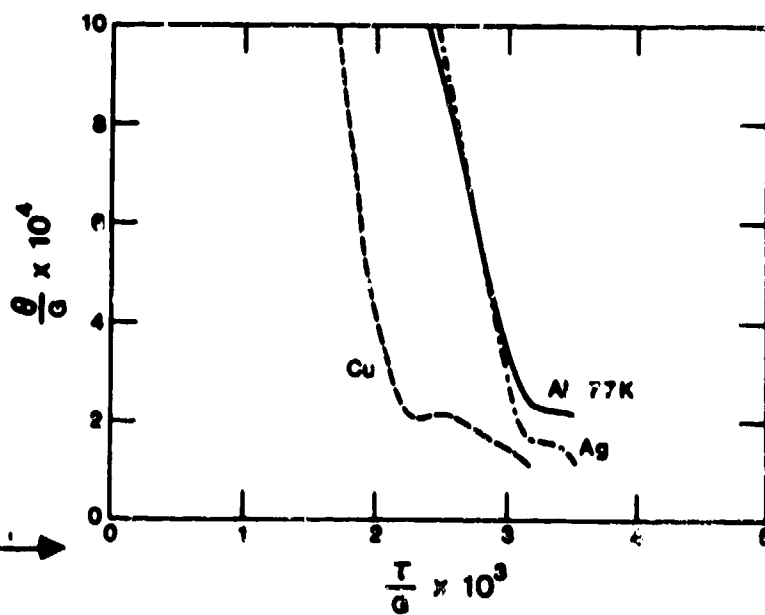

Fig. 4. Hardening rate versus stress in resolved quantities for Al (77 K), Cu (298 K) and Ag (298 K).

The effect of temperature on Stage IV was investigated by performing torsion tests at 77K, 298K, 373K and 473K. Figures 5 and 6 show the results for a commercial purity aluminum and a Al-1%Mg alloy, respectively. The commercial purity aluminum only shows a distinct Stage IV at the lowest temperature although the room temperature behavior suggests that a residual Stage IV is still present. The Al-1Mg alloy, however, shows a clear Stage IV at all temperatures except the highest, both in terms of a sharp transition from III to IV and an extended linear hardening. The flow stresses reached in the alloy are much higher at large strains than those for the corresponding temperatures in the commercial purity material. This shows that small differences in yield strength caused by solute hardening are magnified by strain hardening. Another important observation is that the rate of hardening in Stage IV is similar in all alloys, which is in agreement with previous work (Hughes, 1986, Rack and Cohen 1970 and Alberdi, 1984).
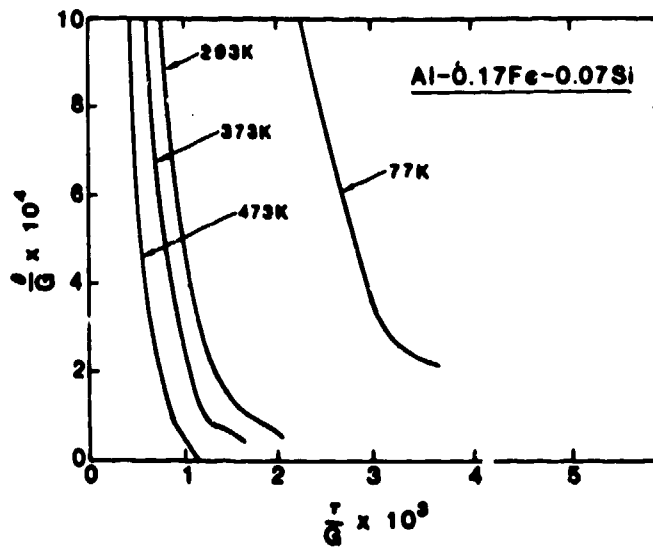

Fig. 5. Hardening rate versus stress for commercial purity aluminum
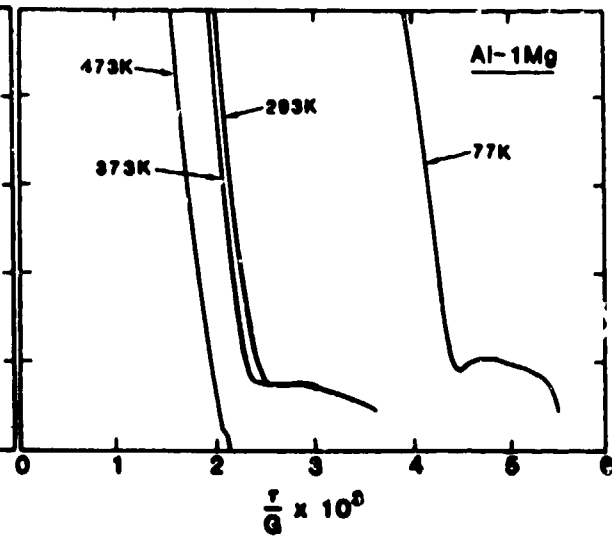

Fig. 6. Hardening rate versus stress for Al-1Mg.
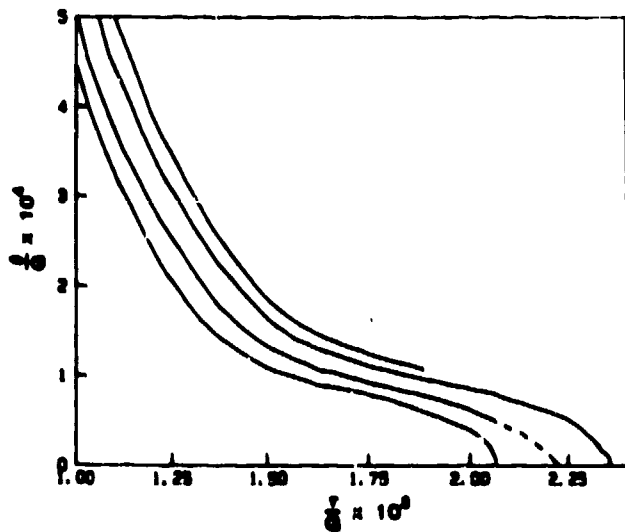

Fig. 7. Hardening rate versus stress for commercial purity Al tested at room temperature at strain rates from 6.9.10⁻¹ (top curve) to 6.9.10⁻⁴ (bottom).
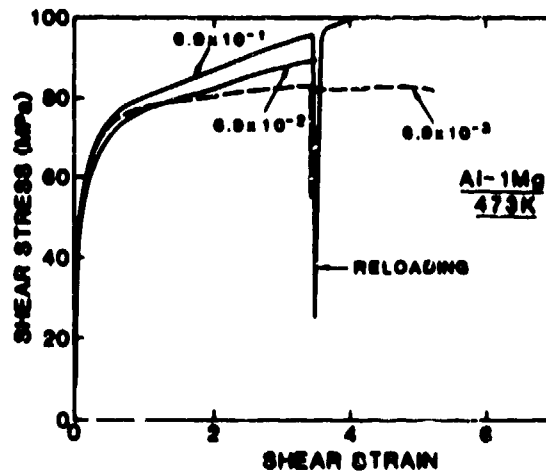

Fig. 8. Shear stress versus shear strain for Al-1Mg tested at various (shear) strain rates at 473K.

The effect of strain rate on strain hardening was investigated by performing torsion tests at different constant strain rates at various temperatures (Rollett, 1987). Stage IV in commercial purity aluminum at room temperature, Fig. 7, appears to be little affected by strain rates that vary over four orders of magnitude. This suggests that the strain rate sensitivity of Stage IV is comparable to that at smaller strains and tests at other temperatures and on other materials suggest the same conclusion. An exception to this, however, occurs when the test temperature is high enough for bulk diffusion to be significant. For Al-1Mg tested at 473K, Stage IV is absent at strain rate of 4.10^{-3} but present at 4.10^{-1}. Smallman and Westmacott (1972) have noted that at this temperature and above, dislocations loops recover rapidly.

MODELS FOR STAGE IV

Again we distinguish two-phase materials from single-phase materials in constructing models for strain hardening in Stage IV. The experimental difference is between a rising hardening rate as observed in two-phase materials and a constant (or decreasing) hardening rate as seen for single-phase materials.

Two-Phase Material model

Two-phase behavior has been modeled on the basis of a Hall-Petch analysis (Embury and Fisher, 1966) and by considering the effects of compatibility strains at the interfaces between the phases (Courtney and Funkenbusch, 1985). This leads to an exponential variation of stress with strain at large strains. The same relation can also be obtained by treating the spacing of the second phase particles as determining the mean free path length of dislocations at large strains such that

$$d\rho/d\varepsilon = k \, d^{-1} \tag{1}$$

where ρ is the dislocation density, k is a constant containing the geometry of the storage process and d is the spacing of the second-phase particles. This relation is analogous to that used to estimate the hardening rate in Stage II (Kocks, 1984). Using the standard relation between flow stress and dislocation density, $\sigma = M\alpha Gb\sqrt{\rho}$, and assuming that for the case of tension that the second-phase particle spacing will go as $d = d_0 \exp(-\varepsilon/2)$.

$$2 \sigma \, d\sigma/d\varepsilon = (M\alpha Gb)^2 \, k \, d_0^{-1} \, \exp(\varepsilon/2) \tag{2}$$

This is rearranged and integrated to give

$$\sigma = \sqrt{2(M\alpha Gb)^2 \, k \, d_0^{-1} \, \exp(\varepsilon/2) + A} \tag{3}$$

where A is a constant of integration. Setting $B = 2(M\alpha Gb)^2 \, k \, d_0^{-1}$ and differentiating.

$$d\sigma/d\varepsilon = B \, \exp(\varepsilon/2) \, / \, \sqrt{(A + B \exp(\varepsilon/2))} \tag{4}$$

In the limit of large strain $B \exp(\varepsilon/2) >> A$ and

$$d\sigma/d\varepsilon \approx \sigma/4 \tag{5}$$

This results in a hardening rate that increases with stress as observed experimentally.

Debris Accumulation from Dynamic Recovery model (DADR)

The model for Stage IV presented here is based on the generally observed fact that plastic straining at low temperatures leads to the accumulation of dislocation debris such as dipoles and loops (Fourie and Murphy), in addition to the dislocation monopoles, which are usually arranged in tangles or cell walls. The accumulation of dipolar debris may occur as part of the glide process and it may occur as part of the dislocation rearrangements due to dynamic recovery. However, the rate of dislocation rearrangement inside the tangles or loose cell walls may well be affected by the debris left there as a consequence of previous rearrangement processes. This effect is the basis of our model.

The mechanism of dynamic recovery has been discussed in detail by Kocks (1984). The tangles, which were originally formed by statistical storage of mobile dislocations, have forward internal stresses within them that lead to rearrangement or even annihilation of dislocation segments in this region, thus gradually transforming the tangle into a cell wall. The rate of rearrangement depends on the relative magnitudes of the total local stress and local resistance, such as the breaking strength of attractive junctions as modified by thermal activation. The latter quantity has the effect of a "saturation stress": when the total local stress is equal to it, no further net accumulation can occur. It is this "saturation stress" (defined in the monopole structure) which may be affected by local dislocation debris accumulation.

A useful starting point for a quantitative model is the Voce description of hardening in Stage III,

$$\theta = \theta_0 (1 - \tau/\tau_{s1}) \tag{6}$$

where θ is the hardening rate, θ_0 is the hardening from geometrical storage of dislocations (Kocks, 1984), τ is the resolved flow stress and τ_{s1} is the saturation stress that would be obtained by extrapolating low-strain data to a zero work hardening rate. The second term describes the effect of dynamic recovery whereby dislocation line length is lost from the stored dislocation structure. If this process is not perfectly efficient but leads to the formation of dipoles and loops then the accumulation rate for such debris can be written as

$$d\rho_{debris}/d\gamma = f \theta_0 (\tau/\tau_s) (d\tau/d\eta) \tag{7}$$

where τ_s is now a limiting stress for the dislocation structure. The fraction, f, is of the order of 0.07 (Rollett, 1987) based on consideration of dipole capture in dislocation tangles. The key feature of the DADR model for Stage IV is that the dislocation debris generated as a by-product of dynamic recovery affects the "saturation" stress but does not directly affect the flow stress. This means that the limiting flow stress in the material now slowly increases as debris is deposited. This concept has the useful aspect that at high enough temperatures, such debris should recover rapidly enough (Rollett, 1987) that it cannot affect the stress, hence Stage IV should disappear, as indeed is observed. Writing the limiting flow stress in the tangles as

$$\tau_s = \alpha G b \sqrt{(\rho_{dis1} + \rho_{debris})} \tag{8}$$

which can be differentiated to give

$$d\tau_s/d\rho_{debris} = 0.5 \alpha G b (\rho_{dis1} + \rho_{debris})^{-0.5} \tag{9}$$

Assuming that $d\tau_s/d\gamma = d\tau_s/d\rho_{debris} \times d\rho_{debris}/d\gamma$ then

$$d\tau_s/d\gamma = f \theta_0 \times \tau^2/\tau_s^2 \tag{10}$$

but in Stage IV, the flow stress is nearly equal to the limiting stress, τ_s. Therefore

$$d\tau_s/d\gamma = f \theta_0 \tag{11}$$

This suggests that Stage IV will intervene at, and remain constant at 0.07 of the Stage III work hardening rate or 3.10^{-4} of the shear modulus. This is in reasonable accord with the experimental observation of Stage IV at 2.10^{-4} of the shear modulus.

CONCLUSIONS

Stage IV is found to occur universally in cubic metals at low enough temperatures and the hardening rate is typically about 2.10^{-4} G in resolved quantities which is low but sufficient to raise the flow stress significantly after large strains. A model has been developed for single phase metals that is based on the accumulation of dislocation debris affecting the effective saturation stress of the material. Two-phase metals also show Stage IV but the hardening behavior is different and they can be modeled on the basis of the dislocation mean free path being controlled by the spacing of the second phase.

ACKNOWLEDGEMENTS

REFERENCES

Alberdi, J. M. G. (1984). Ph.D. thesis, Univ. Navarra, Spain.
Diehl, J. (1956). Z. Metall., 47, 331.
Embury, J. D. and Fisher, R. M. (1966). Acta Met., 14, 147-159.
Fourie, J. T. and Murphy, R. J. (1962). Phil. Mag., 7, 1617.
Funkenbusch, P. D. and Courtney, T. H. (1985). Acta Met., 33, 913-922.
Hecker, S. S. and Stout, M. G. (1982). Deformation, Processing and Structure, ASM, Metals Park.
Hughes, D. A., Gibeling, J. C. and Nix, W. D. (1986). Proc. ICSMA-7, Montreal, Canada, 41.
Kocks, U. F. (1984). Proc. Dislocations and the Properties of Real Materials, Metals Society, London, England, 125.
Kovacs, I. and Feltham, P. (1963). Phys. Stat. Sol., 3, 2379.
Langford, G. and Cohen, M. (1969). Trans. ASM, 62, 623.
Rack, H. J. and Cohen, M. (1970). Mat. Sci. & Eng., 6, 320-326.
Rollett, A. D., Kocks, U. F. and Doherty, R. D. (1986). Formability and Metallurgical Structure, TMS-AIME, Warrendale, 211.
Rollett, A. D. (1987). Ph.D. thesis, Drexel Univ., Pennsylvania.
Smallman, R. E. and Westmacott, K. H. (1972). Mat. Sci. & Eng., 9, 249.
Voce, E. (1948). J. Inst. Metals, 74, 537-562.